Available online at www.sciencedirect.com

ScienceDirect

Physics Procedia 61 (2015) 627 – 632

Physics Procedia

Search for a diffuse flux of cosmic neutrinos with ANTARES

J. Schnabel for the ANTARES collaboration[a]

[a]*Erlangen Center for Astroparticle Physics, Erwin Rommel Str. 91058 Erlangen, Germany, jutta.schnabel@fau.de*

Abstract

The ANTARES neutrino telescope, situated off the French coast at about 2.5 km depth in the Mediterranean Sea, is optimized to detect charged leptons induced by neutrinos in the TeV range. Since its full deployment in 2008, modelling and reconstruction of neutrino-induced event signatures have been introduced and developed to obtain a high degree of accuracy. In this work, muon track directional and energy reconstruction have been applied to four years of ANTARES data in the search for a diffuse flux of astrophysical neutrinos from the charged-current interactions of ν_μ. Reaching a sensitivity which well surpasses the sensitivity of previous ANTARES analyses, a best upper limit of $\Phi_{\nu+\bar{\nu},90\%C.L.}E^2 = 5.1 \times 10^{-8}$ GeV sr^{-1} s^{-1} cm^{-2} can be set.

Selection and peer review is the responsibility of the Conference lead organizers, Frank Avignone, University of South Carolina, and Wick Haxton, University of California, Berkeley, and Lawrence Berkeley Laboratory

Keywords: ANTARES, diffuse neutrino flux

1. Introduction

During the last year, the search for astrophysical neutrinos has gathered momentum through the discovery of a high-energy diffuse neutrino flux of extraterrestial origin in the PeV range by the IceCube collaboration [1]. This sheds first light on the expectations from production mechanisms of high-energy neutrinos in the acceleration regions of astrophysical sources. The detection of those high-energy neutrinos is only feasible in very large volume Cherenkov detectors using naturally abundant material like ice or water. The ANTARES telescope, installed in the Mediterranean Sea and running in its final configuration since 2008, is optimized for the detection of high-energy neutrinos. ANTARES was able to set the then strictest limit on the diffuse astrophysical neutrino flux during the first years of its data taking [2]. Since then, event-selection algorithms and reconstruction methods have improved such that together with the increased quantity of data, a significant increase in sensitivity towards the astrophysical neutrino flux is achieved. The results of two analyses covering the charged-current ν_μ-channel are presented here.

2. The ANTARES Detector

2.1. Detector Layout

The ANTARES detector[3] is located near Toulon, 40 km off the French coast at a depth of 2475m. It consists of 885 Optical Modules (OMs), glass-spheres of 17" diameter which each contains a 10" photomultiplier tube and readout electronics. The OMs are grouped in threes along 12 detection lines of about 480 m length as depicted in Figure 1a, and are facing downwards at an angle of 45°. The detection lines are anchored to the sea bottom by the Bottom String Socket and held upright by buoys. Local control modules

Selection and peer review is the responsibility of the Conference lead organizers, Frank Avignone, University of South Carolina, and Wick Haxton, University of California, Berkeley, and Lawrence Berkeley Laboratory

doi:10.1016/j.phpro.2014.12.062

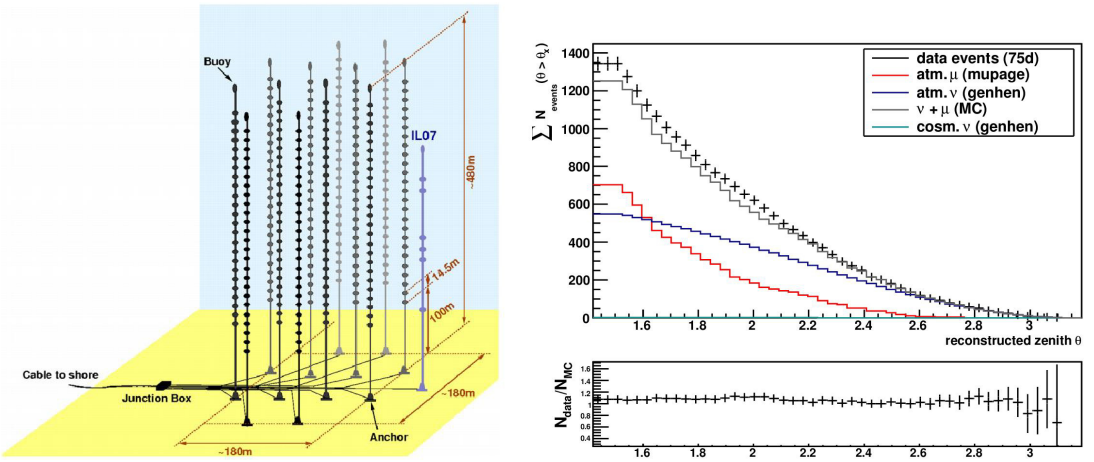

(a) Schematic view of the ANTARES detector

(b) Zenith distribution of events in ANTARES

Fig. 1: a) Schematic view of the ANTARES detector and b) zenith distribution of well reconstructed simulated muon-like events in comparison with data for 75 days of data used for developing these analyses.

ensure data processing and forward the PMT readout along the detection lines towards a common junction box on the seabed which links the detector via an electro-optical cable to the mainland. Onshore, data is triggered, events selected and a first reconstruction performed.
The challenges of an active environment like the deep sea make close monitoring of the environmental conditions mandatory. Therefore, an additional instrumentation line monitors environmental conditions like sea-current, salinity and temperature of the water, and hosts part of an acoustic neutrino detection system and biocams. As the location of the detection lines are subject to the sea current, an acoustic positioning system is employed to locate the individual OMs with a precision better than 10 cm [4], while the timing precision of the PMT readout lies within 2 ns, ensuring individual photon hit measurements within these uncertainties.

2.2. *Event filtering and reconstruction*

The relevant event signatures for the ANTARES detector are produced by neutrino-induced charged leptons with particle energies above a few GeV, which produce Cherenkov radiation at a characteristic angle of 42° along their particle tracks. In the case of a charged-current interaction of high-energy ν_μ, the resulting particle track well exceeds a few meters and can be reconstructed as track-like event, all other event signatures including muon tracks starting in the detector region result in particle cascades and are reconstructed as shower-like events. As photons in the deep sea are also produced by K40-decays and various bacteria which produce single photons through bioluminescence, various trigger algorithms are run on hit selections to identify various types of candidate events, which are then stored for further analysis.
On these triggered events, direction reconstruction assuming a muon track is performed using a likelihood-based minimization method after primary hit selection and track directional estimates [5]. The track reconstruction algorithm calculates an error estimate on the angular resolution of the fit, β, and a likelihood-related parameter Λ which includes, amongst others, the fit uncertainty. Based on this track estimate, the energy of the event can be estimated exploiting the number and arrival time of photons produced by radiative energy-loss processes. As the probability for the occurrence of loss process increases rapidly for muons above a few TeV, their contribution to an event-related hit selection serves as a rough estimate of the particle energy. Various energy estimates are implemented in ANTARES, ranging from a simple count of hits to a dE/dx estimate and reconstruction using artificial neural networks [6]. More details on the operation of the detector and current analyses can be found in a dedicated contribution to this conference [7].

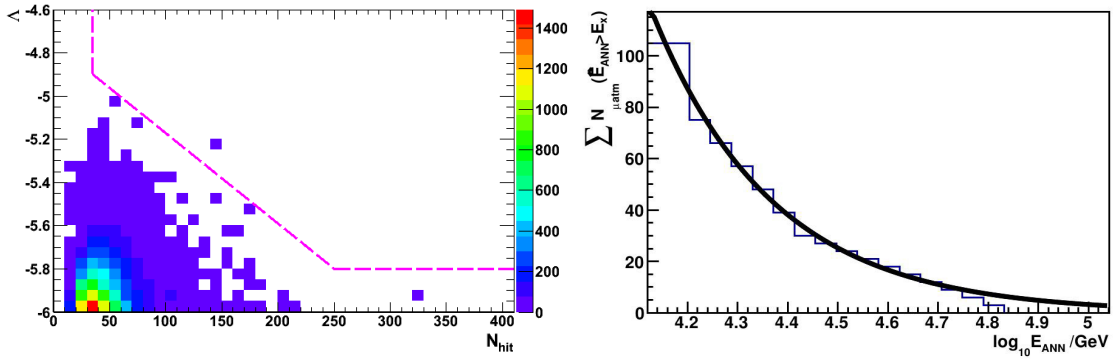

(a) Combined cut on Λ and N_{hits} in analysis A

(b) Extrapolation of $N_{\mu atm}$ in analysis B

Fig. 2: Reduction of the atmospheric muon contribution in analysis A (left) through a combined cut on Λ and N_{hits} for a simulated atmospheric muon sample for 1/3 of the total lifetime, and estimation of the atmospheric muon contribution in analysis B over the energy estimate $\hat{E}_{ANN}$ (right).

3. Searching for a cosmic neutrino flux

Due to the experimental set-up of the neutrino telescope, the search for a diffuse cosmic neutrino flux can be divided into two main steps: Firstly, atmospheric muons entering the detector from above dominate the event sample after initial event triggering by roughly $10^6 : 1$ over the relevant event sample consisting of muon-neutrino events entering the detector from below. These events have to be identified effectively and with high accuracy to optimize the purity of the final event sample. Secondly, an energy estimate has to be employed on the purified event sample to separate the contribution of atmospheric neutrinos from the cosmic flux. Here, the analysis has to favour high-energy events, as cosmic neutrino models predict a much harder spectrum $\propto E^{-2}$ over the atmospheric flux $\propto E^{-3.7}$.
In ANTARES, two analyses were performed on roughly 900 days of data-taking, searching only for events from charged-current ν_μ interactions. These analyses can be seen as complimentary in so far as the first (analysis A) followed a stringent heuristic argumentation for signal optimization as outlined above, while the second (analysis B) chose an inclusive approach to the two analysis steps using a broad scanning of the parameter space for combined muon reduction and signal optimization. Both analyses were developed adopting a blinding procedure with 10% of the data used for the developing of the analysis, which was then applied to the full data sample.

3.1. Event selection

In order to reduce the large amount of data to a manageable size, a first event selection had to be performed by selecting only those events which are well-reconstructed as coming from below the horizon, i.e. with zenith-angle $\theta \gtrsim 90°$. In both analyses, the selection criterion included further a cut on one of the quality parameters Λ and β. These first selection criteria reduce the contribution of atmospheric muons in the event sample by several orders of magnitude, as downward-going atmospheric muons are discarded, and those misinterpreted as upgoing neutrino-induced muons generally show a lower reconstruction quality,

3.2. Suppression of the atmospheric muon background

In this first event sample, a large contribution of atmospheric muons still remains, as can be seen in Figure 1b. From here on, reducing the contribution of atmospheric muons can be viewed as a separate analysis step before optimizing the event selection towards a cosmic signal, as done in analysis A, or as an integrated step in the task of the overall reduction of background events to the cosmic signal events.
In analysis A, a combined cut on the quality parameter Λ and the number of hits selected to be associated with the event was chosen to reduce the number of simulated atmospheric muons to 3, which corresponds

A	$\Lambda(N_{hits})$	$dE/dx > 3.15$	**B**	final sample
N_ν^{WB}	9.4	2.3 ± 0.3	N_ν^{WB}	3.04 ± 0.4
N_ν^{Bartol}	1026	8.4 ± 1.2	N_ν^{Bartol}	4.15 ± 1.1
$N_{\mu\mathrm{atm}}$	4.2	$< 0.4\%$	$N_{\mu\mathrm{atm}}$	4.2 ± 1.0
N_{data}	1422	8	N_{data}	12

Table 1: Event numbers for cosmic neutrinos and atmospheric neutrinos [9] for both analyses after the various selection cuts. The test flux for N_ν^{WB} is $\Phi_{\nu+\bar{\nu}}E^2 = 2 \times 10^{-8}\,\mathrm{GeV\,sr^{-1}\,s^{-1}\,cm^{-2}}$[10].

to one simulated event with weight 3 seen in Figure 2a. An extrapolation over the distribution of $\Lambda(N_{hits})$ for the simulated muon sample was then used to arrive at an extrapolated atmospheric muon contribution of 4.2 events after this cut.
In analysis B, the signal optimization included the estimate of the atmospheric muon contribution as an integral step of the parameter scanning. Here, various parameters were tested as event selection parameters. For each such parameter x, the distribution $N_{\mu atm}(x)$ was used to extrapolate the contribution from atmospheric muons for a given cut on this parameter, see Figure 2b. The overall contribution for a set of cuts was then derived as the mean of all extrapolations $N_{\mu atm} = \sum_{i=0}^{n_{\mathrm{param}}} N_\mu(x = x_{\mathrm{select}})/n_{\mathrm{param}}$.

3.3. Signal optimization

In order to optimize the signal expectation, the model-rejection technique [8] was employed. Due to the main separation of atmospheric neutrino background events and any cosmic neutrino signal by particle energy, analysis A used the energy reconstruction parameter dE/dx as an optimization parameter, which is based on the photon excess due to radiative loss processes observed for particles above a few TeV. This resulted in a reduction of the overall background of atmospheric neutrino events to 8.4 events, see Table 1. With this event selection, analysis A reached a sensitivity of

$$\Phi^A_{\nu+\bar{\nu}}E^2 = 4.7 \times 10^{-8}\,\mathrm{GeV\,sr^{-1}\,s^{-1}\,cm^{-2}} \tag{1}$$

Analysis B included various observables and reconstruction parameters of the events to determine an optimal set of event selection criteria by scanning this parameter space. The scanning resulted a combination of three further event selection criteria after the first event selection. Two of these parameters, the energy estimate based on artificial neural networks $\hat{E}_{ANN}$ and use of the photon equivalent of the total charge of the event A_{hits} can herein be seen as equivalent to the dE/dx and N_{hits} selection criteria in analysis A, while the third parameter, the remaining track quality parameter β, mainly reduces the atmospheric muon contamination. With atmospheric muons and atmospheric neutrino events contributing almost equally to the background of the final selection (see Table 1), this optimization procedure resulted in a sensitivity of

$$\Phi^B_{\nu+\bar{\nu}}E^2 = 4.2 \times 10^{-8}\,\mathrm{GeV\,sr^{-1}\,s^{-1}\,cm^{-2}}, \tag{2}$$

demonstrating the potential of a wider scanning approach for the future, where refining the scanning procedure might contribute to a further gain in sensitivity.

3.4. Uncertainties and error estimates

The main systematic uncertainties entering this analysis are the magnitude of the atmospheric muon flux, the modelling of light absorption and scattering properties of the deep sea water and the photon acceptance of the optical modules. In the case of the atmospheric neutrino background, all these uncertainties can be included in the scaling between the modelled and measured flux at the primary cut level. Therefore, in analysis A, the expected number of atmospheric neutrinos in the final selection was scaled to match the excess of measured events at the primary selection level from a sub-sample of 10% of the data.
To estimate the systematic uncertainties on the signal flux, dedicated simulations were used to estimate the effect of diverging light absorption and scattering and OM efficiency on the event reconstruction and

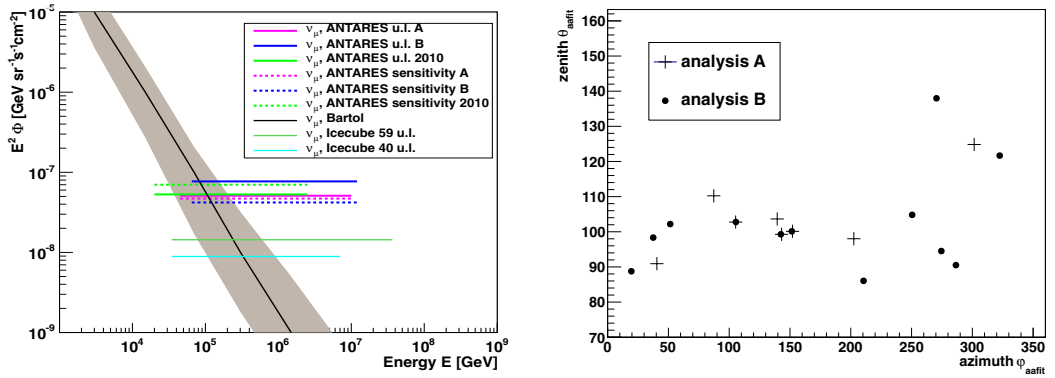

(a) ANTARES sensitivity and limits

(b) Zenith and Azimuth of the final events

Fig. 3: Limits on and sensitivity towards a cosmic neutrino flux of analyses A and B (left); and reconstructed energy (dE/dx-estimate for analysis A, $\hat{E}_{ANN}$ for analysis B) and reconstructed zenith and azimuth angle for events passing the final selection criteria (right)

detection efficiency. The resulting variation of the final event selection number is applied as an uncertainty on the expected signal and neutrino background flux in both analyses.
Finally, as the atmospheric muon contribution in analysis A is reduced below significance, the only error estimate needed on the atmospheric muon contribution is in analysis B, where the variances $\sigma(N_\mu(x = x_{\text{select},i}))$ of the extrapolated atmospheric muon contribution per parameter are introduced as error estimate.

4. Results

All available data taken with the detector in its final 12-line configuration between 2007 and 2011 was analysed. Due to different selection criteria, this resulted in 855 days (A) and 903 days (B) of data. In this sample, analysis A discovered 8 neutrino candidate events while analysis B found 12 muon-like events, of which three events are common between the two analyses. Integrating the systematic errors introduced in the previous paragraph by the method of Conrad et al. [11], this allows the setting of a Feldman-Cousins upper limit at 90 %*C.L.* on the neutrino flux of

$$\Phi^{A}_{\nu+\bar{\nu},90\%C.L.} E^2 = 5.1 \times 10^{-8}\,\text{GeV}\,\text{sr}^{-1}\,\text{s}^{-1}\,\text{cm}^{-2} \quad \text{and} \quad \Phi^{B}_{\nu+\bar{\nu},90\%C.L.} E^2 = 7.7 \times 10^{-8}\,\text{GeV}\,\text{sr}^{-1}\,\text{s}^{-1}\,\text{cm}^{-2} \quad (3)$$

As a statistical overfluctuation is observed in analyis B, it arrives at a less stringent limit despite the higher sensitivity. The different selection criteria lead to slightly different validity ranges of the analysis, for analysis A between 45 TeV and 10 PeV and between 65 TeV and 10 PeV for analysis B. Comparing this result with the previous ANTARES analysis, no improvement in the upper limit could be reached due to an underfluctuation in the previous analysis, which lead to a comparatively stringent upper limit compared to its sensitivity.

5. Conclusion

After four years of data-taking with the full detector, the ANTARES sensitivity towards a cosmic muon-neutrino flux could be increased in comparison to the previous analyses beyond the gain only expected from the statistical increase of data. Two complementary analyses found no significant excess in the data. This result is as expected, as the sensitivity of the analyses did not reach the cosmic neutrino flux discovered by the IceCube collaboration. Assuming the flux cited in [1], these analyses would be expected to find about 1.4 events, which lies within the statistical fluctuation of the analyses. However, a longer run-time of the detector and an inclusion of all neutrino event signatures in ANTARES are expected to further enhance the detection capability of ANTARES towards the cosmic neutrino flux.

References

[1] T. I. Collaboration, Evidence for High-Energy Extraterrestrial Neutrinos at the IceCube Detector, Science 342, 1242856 (2013)arXiv:1311.5238v2, doi:10.1126/science.1242856.

[2] T. A. Collaboration, Search for a diffuse flux of high-energy ν_μ with the ANTARES neutrino telescope, Phys.Lett.B696:16-22,2011arXiv:1011.3772v1.

[3] T. A. Collaboration, ANTARES: the first undersea neutrino telescopearXiv:1104.1607v2.

[4] T. A. Collaboration, The Positioning System of the ANTARES Neutrino Telescope (Jul. 2012). arXiv:1202.3894v3.

[5] A. Heijboer, f. t. A. collaboration, Reconstruction of Atmospheric Neutrinos in Antares (Aug. 2009). arXiv:0908.0816v1.

[6] J. Schnabel, Muon energy reconstruction in the ANTARES detector, Nuclear Inst. and Methods in Physics Research, A (NIMA55282).

[7] M. Spurio, Results from the ANTARES neutrino telescope with six years of data, Contribution to this conference.

[8] G. C. Hill, K. Rawlins, Unbiased cut selection for optimal upper limits in neutrino detectors: the model rejection potential technique, Astropart.Phys. 19 (2003) 393-402arXiv:astro-ph/0209350v1, doi:10.1016/S0927-6505(02)00240-2.

[9] G. D. Barr, T. K. Gaisser, P. Lipari, S. Robbins, T. Stanev, A three-dimensional calculation of atmospheric neutrinos, Phys.Rev.D70:023006,2004arXiv:astro-ph/0403630v1.

[10] E. Waxman, J. Bahcall, High Energy Neutrinos from Astrophysical Sources: An Upper Bound, Phys.Rev.D59:023002,1999arXiv:hep-ph/9807282v2.

[11] J. Conrad, O. Botner, A. Hallgren, C. P. de los Heros, Including Systematic Uncertainties in Confidence Interval Construction for Poisson Statistics, Phys.Rev. D67 (2003) 012002arXiv:hep-ex/0202013v2, doi:10.1103/PhysRevD.67.012002.